ELECTROCHEMICAL PERFORMANCE OF MECHANOCHEMICALLY SYNTHESIZED $La_{0.8}Sr_{0.2}MnO_3$

K. R. Nagde[1] ,S. S. Bhoga[2]
[1]Government Vidarbha Institute of science and humanities, Amaravati, India
[2]Department of Physics, R. T. M. Nagpur University, Nagpur, India,

ABSTRACT

The $La_{0.8}Sr_{0.2}MnO_3$, LSM, was prepared by mechanochemical method using planetary monomill at fixed 600 rpm for different grinding times. The $La_{0.8}Sr_{0.2}MnO_3$ single phase material forms after 7h of grinding/milling time. Furthermore, the phase of the sample was found to be cubic. The agglomeration of nano-crystalline grains was revealed by SEM study. The minimum area specific resistance, ASR, was found for this prepared sample.

Keywords: Mechanochemical synthesis, X-ray powder diffraction, nano-crystallites, scanning electron microscopy, cathode and fuel cell.

I. INTRODUCTION

In recent years much attention has been focused on to lower the temperature of solid oxide fuel cell (SOFC). Lowering the temperature reduces the production cost and increases their cell life [1]. Furthermore, the reduction in working temperature leads to the alteration of their electrochemical performance in terms of density and ionic conductivity of the electrolyte [2]. LSMand yttria- stabilized zirconia, YSZ, has been used as potential cathode and electrolyte materials respectively but have disadvantage with that of thermal expansion coefficient (TEC) [3]. Hence, the more attention has been focused on the development of composite cathode which is nothing but mixture of ionic and electronic conductor material. The advantage of composite cathode over the pure one is that they extent the electrochemical reaction areas by oxy-ion migration through electrode as well as electrolyte. The LSM with gadolinia doped ceria (GDC) composite studied well due to its advantages over the YSZ electrolyte.

The electrochemical performance of cell have influenced by the preparation techniques [4]. Recently, most of the research has been focused on thedevelopment of a low temperature synthesis of cathode material. Mechanochemical synthesis requires lower temperature as compare to that of other conventional technique and leads to a nano-crystalline material. Nanostructured materials have attracted a great deal of attention due to either improved or unique properties. The nano-materials have normally been synthesized by two approaches viz. physical and chemical [5-6]. The former method includes sputtering, ball-milling, evaporation, laser ablation, etc. The latter one encompasses combustion, chemical vapor deposition, thermo-chemical, sol-gel, chemical precipitation, etc. The mechanochemical alloying (MA), belongs to first approach of nano-materials preparation, involves the mixing of initial reagents using high-energy ball mill. The MA technique has also been termed as mechanochemically activated self-propagating high-temperature synthesis (MASHS).

All above factors have promoted us to prepare LSM using low temperature MA alloying technique. Also the effect of MA on the phase formation of LSM as well as on electrochemical performance was studied during the present study.

II. METHODS AND MATERIAL

The MnO_2, La_2O_3 and SrO, Sigma Aldrich with purity > 99.9 %, were used as starting reagents. La_2O_3 was heated at 1000 °C for 12 h so as to remove absorbed H_2O and CO_2

before weighing. On the other hand, MnO_2 was heated at 600 °C for 12 h in order to convert it into Mn_2O_3. Later, the requisite mole fractions of ingredients with and without either salicylic or stearic acid weremixed. Thus obtained mixture was subjected to the milling as described below.

A planetary monomill (Fritsch Pulverisette-6, Germany) was used for the ball milling. The batch of 15 g of the above mentioned mixture was taken into the 80 ml capacity tungsten carbide (WC) bowl. Later 35 WC balls of 10 mm diameters were added into it and closed with a WC lid. The time of the planetary monomill was varied during the grinding so as to optimize it with fixed 600 rpm, rotational speed. Finally, the ground samples, for different times, were subjected to the sintering at 700 °Cfor a fixed duration of 4 h.

All the samples under study were characterized using X-ray powder diffraction, PANalyticalX'pert PRO, Philips, Holland, with curved graphite crystal as a monochromator, and using Cu K_α radiations. The obtained XRD data were profile fitted with the help of X'pertHighscore plus software before indexing. The values of *d* and relative intensity (I/I_0) for LSM obtained with the help of X-pert Highscore plus, and then compared with the standard JCPDS (joint committee on powder diffraction standard). Also, the lattice cell constants were determined using Unit Cell, computer software developed by Holland and Redfern [7]. The crystallite size was determined using X'pertHighscore plus based on Debye Scherer formula (1),

$$t = \frac{0.9\lambda}{\beta \cos\theta_B} \quad (1)$$

where *t*, λ, and $\theta_B$were thickness, X-ray wavelength and Bragg's angle, respectively. Here, β was obtained using formula

$$\beta = \beta_m^2 - \beta_s^2 \quad (2)$$

where, β_m and β_s were measured and standard full width of half maxima (FWHM) of diffracted line, respectively. The β_s was estimated from the XRD pattern obtained by running the experiment on the standard silicon sample provided by Panalytical, Netherlands.

The microstructures of sintered samples were examined with the help of scanning electron microscope, JEOL JSM-6380A.

$Ce_{0.8}Gd_{0.2}O_2$, GDC, nano powder procured from Aldrich, USA was used as an electrolyte for the preparation of composite cathode.For electrochemical investigations, initially the slurry / ink of each cathode composition was obtained as follows. Specifically, 1g batch of $La_{0.8}Sr_{0.2}MnO_3$ and GDC mixed with polyvinyl buteral binder, sodium free corn oil and methyl ethyl ketone. The mixture was ball milled for 5 h with 300 rpm using 20 tungsten carbide balls of 10 mm diameter in Pulversitte-6 monomill. The GDC nano-powder was fired at 800 °C for 2 h. Subsequently, GDC electrolyte was obtained in the form of a circular disc of 9 and 1 - 2 mm diameter and thickness, respectively as discussed above. Later, they were sintered at 1400 °C for 6 h. The density of GDC was about 96% of the theoretical value. The slurry / ink of cathode material was then spin coated on both the flat surfaces of sintered GDC electrolyte at 3000 rpm for 60 S so as to obtain the symmetric cell of configuration given below,

composite cathode / GDC / composite cathode(3)

The symmetric cell was initially baked at 600 °C for 2 h so as to burn out the organic binders, and then finally sintered at 1000 °C for 2 h. The experimental procedures to evaluate electrochemical performance of symmetric cell were similar to those described elsewhere [8].

III. RESULTS AND DISCUSSION

3.1.X-ray powder diffraction

The X-ray powder diffraction patterns of LSM prepared by mechanochemical alloying with milling time, 2, 3, 5, and 7 h are shown in the Figs. 1(a) - (d), respectively. In general, all the diffracted lines were broadened than usual ones. Moreover, it indicated that all the samples are crystalline in nature. The XRD pattern depicted in Fig.1(a) revealed the broadened characteristic diffraction lines only corresponding to initial reagents. No line corresponding to final product i. e. LSM was seen after milling the reagents for 2 h. A close look at Fig.1 (b) also suggested that all the diffracted lines due to initial reagents.

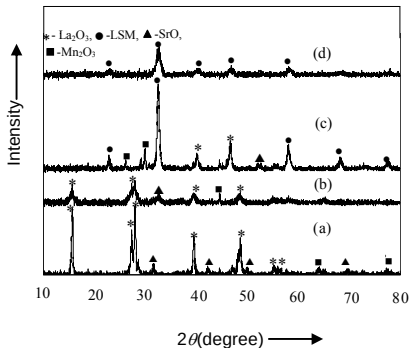

Fig. 1. X-ray diffraction patterns for LSM-Wt with milling time (a) 2h, (b) 3h, (c) 5h and (d)7h.

In Fig. 1 (c) a few number of peaks corresponding to LSM appears. The intensity of diffracted lines due to LSM were seen increasing further with increase in milling time (Fig. 1(c)), whereas, the intensity of lines due to reagents decreases. A close look at the Fig. 1(d) revealed that all the potential characteristic diffraction lines, with small deviation, matched with the JCPDS (joint committee on powder diffraction standard) data (File No. 01-075-0440) corresponding to cubic $LaMnO_3$ on milling reagents for 7 h. No line(s) corresponding to initial reagents or any intermediate compound(s) was seen suggesting complete formation of it in a single phase on milling the reactantsfor 7 h.So, it can be said that purephase LSM forms after milling it for 7h at 600 rpm which was less than that of the reported earlier [9,10].

The X-ray diffraction patterns of LSM sintered at 500°C, 600°C and 700°Care shown in Figs 2 (a-c) respectively.The increased sharpness of the characteristics diffraction lines due to LSMseen in Fig. 2 (a-c) implies further improvement in the crystallinity of ball milled samples after sintering. These results were in line with the general observation that the crystallinity improves with the increase in sintering temperature in case of poor crystalline materials.

A close look at the Fig. 2(a-c) revealed that all the potential characteristic diffraction lines matches with the JCPDS (joint committee on powder diffraction standard) data (File No. 01-075-0440) corresponding to cubic $LaMnO_3$.

From the above results, it can be inferred that the state of microcrystallinity or amorphous like state, necessary for mechanochemical reaction leading to the formation of LSM of reagents, was achieved after milling it. Furthermore, minimum of 7 h milling time with 600 rpm was required for the formation of LSM.Though, merely millng forms the pure phase cubic LSM, sintering at high temperature for long time duration was necessary for the formation of solid solution and for maximum intensity.

The powder particle gets cold-welded to each other due to the heavy plastic deformation experienced by them during milling. The surface active agents adsorbed on the particle surfaces interfere with cold welding and lower the surface tension of solid material [6]. The nature and the quantity of the process control reagents used and the type of powder milled would determine the final shape, size, and purity of the powder particle. Use of the larger quantity of PCA reduces the particle size by 2-3 orders of magnitude[6].Niu has been noted that a homogeneous distribution of particle size could be easily achieved when the PCA is in a liquid state than it is in solid state[11].

The lattice cell constant and crystallite size for LSM sintered at 700°C, are 3.89 ± 0.05(Å) and 864.00±7(Å)respectively.The value of lattice cell constant is matched closely with that of the standard JCPDS values.

3.2 Scanning electron microscopy

Scanning electron microphotographs (SEM) of LSM sintered at 500°C, 600°C and 700°Care displayed in Figs. 3(a-c) respectively.

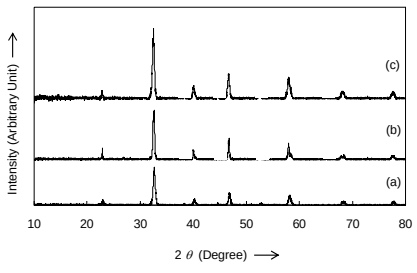

Fig. 2 *X-ray diffraction patterns for sintered LSM at (a) 500 °C, (b) 600 °C and (c) 700 °C.*

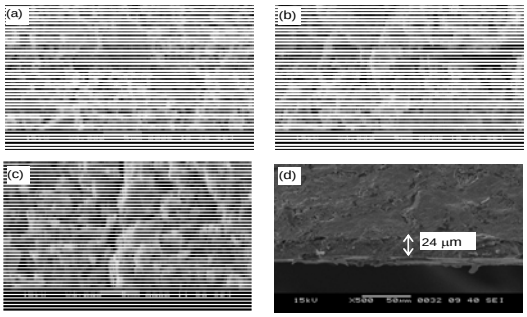

Fig. 3 Scanning electron microphotographs of LSM sintered at (a) 500°C, (b) 600°C, (c) 700°C and (d) electrode / electrolyte interface of Cell

The grains in all the cases are nanocrystalline in nature. Furthermore, agglomerated grains resulted in micro-pores, which were uniformly distributed throughout the samples. The microphotographs of cathode of Cell across the electrode-electrolyte interface are depicted in Fig. 3(d). A close scrutiny of Fig. 3(d) indicated intimate contact across electrode-electrolyte interface. Furthermore, it was homogeneous. The electrode layer thickness was approximately 24μm.

3.4 Electrochemical impedance spectroscopy

Typical electrochemical impedance spectra (EIS) of cell at various temperatures are depicted in Fig. 4. EIS suggested presence of two discernible semicircular arcs.

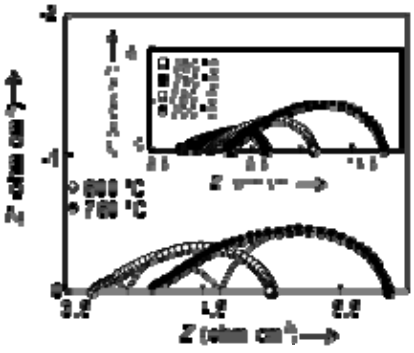

Fig. 4. Complex impedance plots of Cell-II at different temperatures

The impedance spectra were analyzed using computer programme revealed two overlapped semicircular distorted arcs.The presence of two semicircular arcs (dotted curves in the low and the mid frequency regimes) suggested at least two different electrode processes that limited the oxygen reduction reaction. The low and mid frequency arcs were due to oxy ion diffusion and charge transfer process, respectively.

Similar interpretation was done by Suzuki et al and other researchers [12-15]. Chen etal also observed two semicircular arc in low and mid frequency region for LSM on YSZ at 850 °C. The low frequency arc commonly associated with surface diffusion of oxygen. Heuveln et al attributed the mid frequency arc to the charge transfer process [16, 17]. The absence of semicircular arc in the high - frequency region was attributed to the limitations of high frequency of FRA 1255B (≤1MHz). The activation energy E_a=0.93±0.003 eV determined from the Arrhenius plot (log σTVs $10^3/T$) due to bulk electrolyte (R_b) estimated from high frequency domain, is in good agreement with the value for GDC electrolyte reported earlier [18, 19]. The real axis intercepts of all semicircular arcs, as expected, increased with decreased temperature; indicated increased ASR as well as bulk electrolyte resistance.

The electrochemical impedance plots at 700 °C for different oxygen partial pressures (P_{O_2}) around Cell are depicted in Fig. 5.

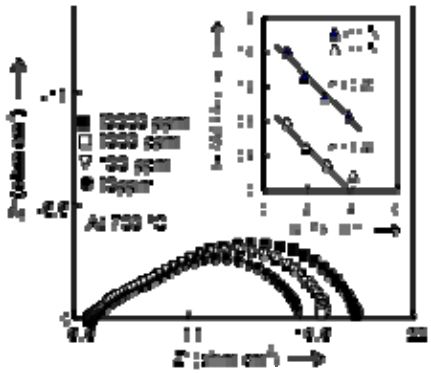

Fig. 5. Complex impedance plots at different oxygen partial pressures for Cell-II at 700 °C and inset shows variation of ASR with oxygen partial

In general, *x*-axis intercept of low frequency semicircular arc increased with decrease in P_{O_2}. On the other hand, the electrolytic bulk resistance / conductivity was least affected inspite of variation in P_{O_2}. The variation of log (ASR) at 600 and 700 °C with log (P_{O_2}) shown in insert of Fig.5 suggested a linear dependence of the former on the latter.

In other words, the ASR varies with the oxygen partial pressure according to the relation given below

$$ASR = ASR_0(P_{O_2})^{-n} \quad (4)$$

The value of *n* was useful to understand the type of species and electrochemical reactions involved in electrode reactions [20].

$n = 1$, $O_2(g) \rightleftarrows O_{2,ads}$

$n = 0.5$, $O_{2,ads} \rightleftarrows 2O_{ads}$

$n = 0.25$, $O_{ads} + 2e' + V_O^{\bullet\bullet} \rightleftarrows O_O^x$

$n = 0.25$, $O_{ads} + 2e' + V_O^{\bullet\bullet} \rightleftarrows O_O^x$

The n = 0.22 at 700 °Cwas generally consider to be the charge transfer process represented by

$$O_{ad} + 2e' + V_O^{\cdot\cdot} \rightarrow O_O^x$$

where O_{ad}, $V_O^{\cdot\cdot}$ and O_O^xwere an adsorbed oxygen atom on electrode, oxygen ion vacancy and oxygen ion in normal lattice site, respectively[21].

IV. CONCLUSIONS

The $La_{0.8}Sr_{0.2}MnO_3$was prepared using mechanochemical method at different timing for fixed 600 rpm. Pure phase cubic LSM was prepared after milling it at 7h. The area specific resistance for Cell was found 0.60 ohm cm^2. The n = 0.22 at 700 °C was considered as a rate limiting step.

V. REFERENCES

[1] M. Ferkhi, S. Khelili, L. Zerroual, A. Ringuede, M. Cassir, Electrochim.Acta 54 (2009) 6341.

[2] E. Ivers-Tiffée, A.Weber, D. Herbstritt, J. Eur. Ceram. Soc. 21 (2001) 1805

[3] M. Zhang, M. Yang, Z. Hou, Y. Dong, M. Cheng, Electrochim. Acta 53 (2008) 4998

[4] K. R. Nagde, S. S. BhogaElectrochem. Soc. (accepted)

[5] A. P. Khandale, S. S. Bhoga, Integrated Ferroelectrics 116 (2010) 59.

[6] C. Suryanarayana, Progress in materials science 46 (2001)1.

[7] T. J. B. Holland, S. A. T. Redfern, Mineral Mag. 61 (1997) 77.

[8] A. P. Khandale, S. S. Bhoga, J. Power sources 195 (2010) 7982.

[9] K. R. Nagde, S. S. Bhoga, Ionics 16 (2010) 361.

[10] Q. Zhang, T. Nakagawa, F. Saito, J. Alloys and Comp. 308(2000) 121.

[11] X. P. Niu, PhD thesis, Katholieke University, Leuven, Belgium (1991)

[12] G. J. Li, Z. R. Sun, H. Zhao, C. H. Chen, R. M. Ren, Ceram. Int.33 (2007) 1503.

[13] S. P. Jiang, W. Wang, Solid State Ionics 176 (2005) 1185.

[14] R. V. Wandekar, B. N.Wani, S. R. Bhardwaj, Solid State Sci.11 (2009) 240

[15] T. Suzuki, M. Awano, P. Jasinski, V. Petrovsky, H. Anderson, Solid State Ionics 177 (2006) 2071.

[16] X. J. Chen , K. A. Khor, S. H. Chan, Solid State Ionics (167) (2004) 379

[17] F. H. van Heuveln, H. J. M. Boulomeestor, F. P. F. van Berkel, J. electrochem. Soc. 144 (1997)134.

[18] A. P. Khandale, S. S. Bhoga, Electrochim.Acta56 (2011) 9219.

[19] K. Singh, S. A. Aacharya, S. S. Bhoga, Ionics 12 (2006) 295.

[20] S. Ping, L. Qiang, H. Hua, Z. Hui, Z. Ying, L. Nan, J. Viricelle, C. Pijolat J. Power Sources 196 (2011) 5835.

[21] O. J. Velle, T. Norby, P. Kosfstad, Solid State Ionics 47 (1991) 161.